Oxidation state determination of plutonium aquo ions using x-ray absorption spectroscopy

9 AUTHORS, INCLUDING:

Steven D. Conradson
SOLEIL synchrotron
241 PUBLICATIONS **7,103** CITATIONS

SEE PROFILE

Ilham Almahamid
New York State Department of Health
45 PUBLICATIONS **263** CITATIONS

SEE PROFILE

David L Clark
Los Alamos National Laboratory
237 PUBLICATIONS **5,488** CITATIONS

SEE PROFILE

Pergamon

PII: S0277–5387(97)00287–8

Oxidation state determination of plutonium aquo ions using x-ray absorption spectroscopy

Steven D. Conradson,[a]* Ilham Al Mahamid,[b] David L. Clark,[c,d]
Nancy J. Hess,[e] Eric A. Hudson,[b] Mary P. Neu,[c,d] Phillip D. Palmer,[c]
Wolfgang H. Runde[d,f] and C. Drew Tait[c,d]

[a]Chemical Science and Technology Division and the Materials Science and Technology Division, Los Alamos National Laboratory, Los Alamos, NM 87545, Mail Stop D-429, U.S.A.

[b]The Lawrence Berkeley National Laboratory, Berkeley, Mail Stop 70A-3317, CA 94550, U.S.A.

[c]Chemical Science and Technology Division and the Materials Science and Technology Division, Los Alamos National Laboratory, Los Alamos, NM 87545, Mail Stop G-739, U.S.A.

[d]The G. T. Seaborg Institute for Transactinium Science, Livermore, CA, U.S.A.

[e]The Materials Science Division, Pacific Northwest Laboratory, Richland, WA 99352, Mail Stop K2-44, U.S.A.

[f]Chemical Science and Technology Division and the Materials Science and Technology Division, Los Alamos National Laboratory, Los Alamos, NM 87545, Mail Stop J514, U.S.A.

Abstract—Four oxidation states (III, IV, V, and VI) of Pu may coexist under environmentally relevant conditions. An efficient method to determine the states actually present in various matrices would enhance the ability to model the fate and transport of plutonium in process streams and in the environment. This communication establishes that the L_3 X-ray absorption near-edge structure (XANES) spectra of Pu are primarily determined by the valence state and the presence or absence of the trans dioxo moiety, consistent with previous U and Np XANES studies. The edge energies were observed to shift progressively to higher energy with increasing valence, with an average 1.68 eV increase per formal oxidation state increase. In addition, the general spectral shape of the (III) and (IV) species is clearly different from the dioxo-containing (V) and (VI) species, with the first maximum much larger and sharper for the (III) and (IV) spectra than for the (V) and (VI) spectra. © 1998 Elsevier Science Ltd. All rights reserved

Chemical speciation, as the determinant of reactivity of the key radionuclides in nuclear waste (Sr, Cs, U, Np, Pu, Am, and Tc), is critical towards understanding and predicting their fate and transport in the environment [2–6]. The number of accessible oxidation states for transuranic ions in aqueous solution adds to the complexity of their chemistry. For plutonium, four oxidation states (III, IV, V, and VI) may coexist in aqueous solution [7]. X-ray absorption near-edge structure (XANES) spectroscopy is an established technique for the determination of oxidation state and local chemical environment, even at relatively low concentrations and without requiring extensive sample preparation that could induce artifacts [8]. The determination of edge energies and near-edge features of known Pu aquo species for different oxidation states will allow the determination of predominant oxidation states in complex matrices such as solution/solid-surface interfaces, amorphous solids, or radioactive tank wastes [9]. While XANES spectra of U and the complete suite of accessible Np oxidation states have been reported [10,11], there have been no systematic studies performed for Pu. We report here

---

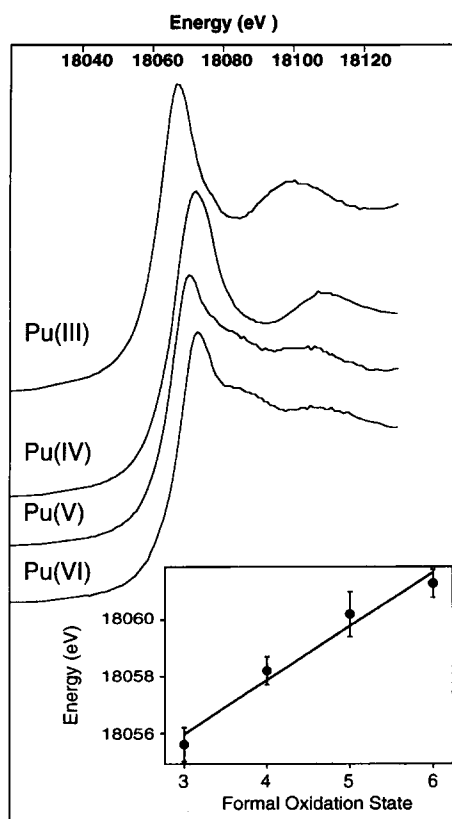* Author to whom correspondence should be addressed.

Fig. 1. Plutonium XANES spectra for the aquo (III), (IV), (V), and (VI) species. The edge energies, as measured by the inflection point of the arctangent part of the fits, are inset.

the edge energies and near-edge features for plutonium aquo ions in oxidation states (III–VI).

Aqueous plutonium solutions containing a single oxidation state were prepared electrochemically [12], and the stability of the stock solutions was verified both before and after XANES analysis with UV–vis–NIR absorption spectroscopy. Each stock solution contained greater than 98% of a single plutonium species, although any effect of the X-ray beam on

the actual sample was not directly addressed. Similar chemical environments around each of the plutonium cations were produced by preparing and studying the aquo complexes. Aquo ions of Pu^{3+}, Pu^{4+}, and PuO_2^{2+} were prepared in 1 M $HClO_4$, while PuO_2^+ was prepared in perchlorate solution at pH 3 and subsequently stabilized with respect to disproportionation by adjusting the pH of the solution to 6 [12]. X-ray absorption measurements were performed in transmission ($Pu^{III,IV,VI}$) or fluorescence (Pu^V) mode at the Pu L_3-edge [13] and calibrated against a Zr foil [14]. The energies of the Pu absorption edges were determined in two ways: (1) as the inflection point of the edge and (2) as the energy of the arctangent in least squares fits of the XANES region using an arctangent plus Gaussian functions [15]. In the latter case, the arctangent represents the $2p_{3/2} \rightarrow$ continuum transition, and thus coincides with the onset of the absorbance, while the Gaussians fit the higher order features, including the main peak and the first EXAFS oscillations. The initial peak, or 'white line', has historically been assigned to the allowed bound final state $2p_{3/2} \rightarrow 6d$ transition [10,11,16,17], but recent work suggests that it may be better explained as EXAFS. A theoretical analysis of the transition will be reported elsewhere [18]. The type of fits described here are comparable to XANES fits reported for U and Np [10,11,16,17].

Pu L_3 edge spectra of the aquo ions are shown in Fig. 1, where significant shifts to higher energy with increasing valence are observed. In addition, the general shape of the near edge spectra for the (III) and (IV) species is clearly different from those of the dioxo-containing (V) and (VI) species (Fig. 1). Specifically, the main peak is much more distinct for the (III) and (IV) spectra, whereas the (V) and (VI) spectra exhibit a prominent shoulder on the high energy side of this peak. These characteristics are similar to the L_3 XANES of $U^{IV,VI}$ and $Np^{III-VII}$ [10,17]. The energies of the edge and 'white line' positions are listed in Table 1. The edge energy shifts determined by the second derivatives generally increase with the formal oxidation state of the absorbing metal atom, such that

Table 1. XANES data for plutonium aquo complexes in different oxidation states[a]

Sample	2nd der. crossing	Arctan			Gaussians		
		edge	height	width	1st	2nd	3rd
Pu^{3+}	18060.1	18055.6 ± 0.6	0.339 ± 0.006	0.19 ± 0.02	18064.0	18070.3	—
Pu^{4+}	18063.2	18058.2 ± 0.5	0.337 ± 0.005	0.19 ± 0.03	18068.3	18075.6	—
PuO_2^+	18062.6	18059.7 ± 0.2	0.322 ± 0.005	0.23 ± 0.03	18067.3	18071.6	—
PuO_2^+	18062.6	18060.2 ± 0.8	0.327 ± 0.004	0.15 ± 0.02	18065.7	18072.1	18099.8
PuO_2^{2+}	18064.8	18061.3 ± 0.5	0.323 ± 0.007	0.22 ± 0.02	18068.9	18078.4	—
PuO_2^{2+}	18064.8	18061.2 ± 0.6	0.321 ± 0.005	0.18 ± 0.03	18068.9	18080.0	18103.2

[a] All energy positions are in eV, where the energy axis had been calibrated using the XANES edge from Zr foil at 17,999.35 eV. The arctan height, width, and edge are taken from variables k[1], k[2], and k[3], respectively, as defined in ref. [13].
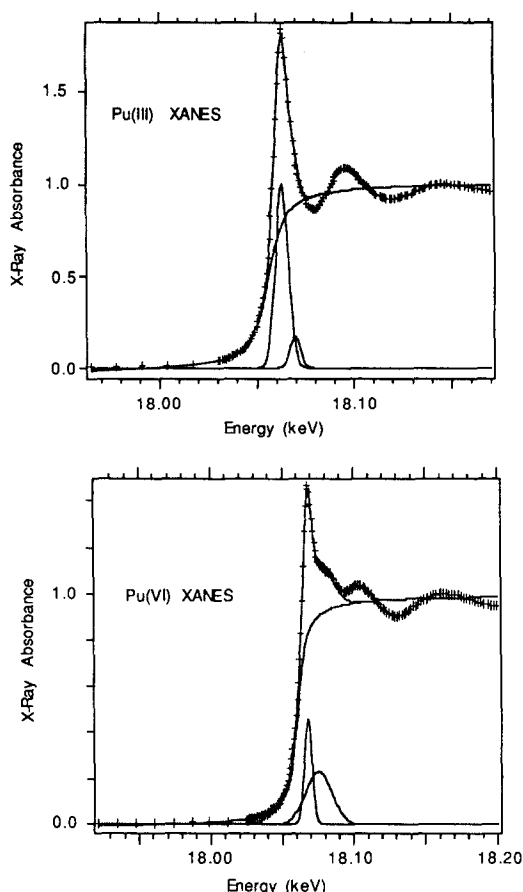
Fig. 2. Representative fits of the XANES for Pu[III] and Pu[VI], representing the aquo- and dioxo-containing species, respectively.

ference from the 'white line' when determining the energy of the edge.

This work shows that the primary determinants of Pu XANES are the valence state and the presence or absence of the trans-dioxo moiety, consistent with previous U and Np XANES studies [16,17,19,20]. Furthermore, this work establishes that XANES spectroscopy provides a rapid and straightforward means for determination of the average valence of Pu in species with primarily oxygen ligation, using a combination of the spectral features (III and IV vs V and VI) and the calculated arctangent edge energy. We anticipate that these findings will aid in our ability to determine the oxidation state of Pu in a variety of important complex chemical matrices such as aging radioactive wastes, process stream residues, glasses, ceramics, and soils.

Supplementary data—Figures of the fits for all 4 Pu oxidation states is available. Ordering information is given on any current masthead page.

(III), (IV/V), and (VI) are readily distinguished (Table 1). We note that while the overall shapes of the near edge spectra for (IV) and (V) states allow unambiguous assignment, their energies as determined by using only 2nd derivatives are quite similar. If the trend in edge shift reflects the charge, this might be explained by the increase in covalency (and diminution of difference in Pu charge) associated with the presence of the dioxo moiety in (V) and (VI) states. However, when fit to an arctangent and 2 Gaussians (Fig. 2), [15] which might be more sensitive to valence and less so to the positions and shapes of the other features of the edge, the arctangent (ionization) energies do increase progressively with formal oxidation state. The inset of Fig. 1 shows the excellent linear correlation between the arctan-based edge position and Pu oxidation state ($r^2 = 0.997$). Addition of a third Gaussian to the XANES deconvolution for the (V) and (VI) species affected the edge position only marginally (Table 1), and the general conclusion of higher edge position with oxidation state remains. Therefore, the arctangent fitting strategy avoids inter-

REFERENCES

1. (a) LANL Mailstop D429; (b) LBNL Mailstop 70A-3317; (c) LANL Mail Stop G739; (d) G. T. Seaborg Institute; (e) PNNL Mailstop K2-44; (f) LANL Mailstop J514.
2. Dozol, M. and Hagemann, R., *Pure and Appl. Chem.*, 1993, **65**, 1081.
3. Clark, D. L., Hobart, D. E. and Neu, M. P., *Chem. Rev.*, 1995, **95**, 25.
4. Kim, J. I., *Mater. Res. Soc. Symp. Proc.*, 1993, **294**, 3.
5. (a) Fuger, J., *J. Nucl. Mater.*, 1993, **201**, 3; (b) Choppin, G. R., *Radiochim. Acta*, 1983, **32**, 43.
6. Hobart, D. E., *Proc. Robert A. Welch Conf. Chem. Res.*, 1990, **34**, 379.
7. Weigel, F., Katz, J. J. and Seaborg, G. T., *The Chemistry of the Actinide Elements*; (Katz, J. J., Seaborg, G. T. and Morss, L. R., eds) Vol. 1, 781, Chapman and Hall, London (1986).
8. Bianconi, A., *X-Ray Absorption: Principles, Applications, Techniques of EXAFS, SEXAFS and XANES*; Koningsberger, D. C. and Prins, R., Eds., Vol. 92, 573, John Wiley & Sons: New York (1988).
9. Brown, G. E., *Mineral–Water Interface Geochemistry*; Hochella, M. F. and White, A. F.,

Eds; Vol. 23; 309, Mineralogical Society of America, Washington, D.C. (1990).

10. Morris, D. E., Allen, P. G., Berg, J. A., Chisholm-Brause, C. J., Conradson, S. D., Donohoe, R. J., Hess, N. J., Musgrave, J. A. and Tait, C. D., *Environ. Sci. Techn.*, 1996, **30**, 2322.

11. Bertram, S., Kaindl, G., Jove, J. and Pages, M., *Physica B*, 1989, **158**, 508.

12. ^{242}Pu was purified using ion chromatography (Lewatit MP-500) of Pu^{VI} in 9 M HCl (PuCl$_6^{2-}$), and eluted using 0.5 M HCl. Purified Pu^{IV} was oxidized to Pu^{IV} in fuming HClO$_4$, and the resulting solution diluted with 1 M HClO$_4$, and analyzed spectrophotometrically at 830 nm ($\varepsilon = 525$ M^{-1} cm^{-1}). Pu^V was prepared by placing Pu^{VI} in 0.2 M ClO$_4$, adjusting the pH to 3 using NH$_4$OH, followed by electrochemical reduction at a potential of 0.54 V (*vs* SCE). The pH was adjusted to 6, and the solution analyzed spectrophotometrically at 569 nm ($\varepsilon = 19$ M^{-1} cm^{-1}). Pu^{III} solutions were obtained by electrolytic reduction of Pu^{VI} at 0.51 V (*vs* SCE) in 1 M HClO$_4$, and analyzed spectrophotometrically at 600 nm ($\varepsilon = 37.5$ M^{-1} cm^{-1}). The Pu^{III} solution was oxidized electrochemically to Pu^{IV} at 1.2 V (*vs* SCE) in 1 M HClO$_4$. At this potential, Pu^V and Pu^{VI} could form, but the rate of formation for such irreversible reactions is small. Pu^{IV} is analyzed spectrophotometrically at 470 nm ($\varepsilon = 56.5$ M^{-1} cm^{-1}). Final Pu solution concentrations were 0.10 M for all samples except for Pu^V, which was 0.008 M.

13. XANES data were recorded at 295 K at the Stanford Synchrotron Radiation Laboratory (SSRL): unfocused beamline 4-2, Si(220), double-crystal monochromator, 3.0 GeV, 60–100 mA. The XANES region was taken as extending above the Pu edge to 18,120 eV.

14. The Pu L$_3$ edge spectrum normalized by setting the value of a polynomial fit through the pre-edge region to zero and that of a polynomial fit through the EXAFS region to unity at 18,120 eV. The spectra were calibrated by comparison of spectra for Zr foil, where the first inflection point was defined to be 17,999 eV.

15. Fit = k[0] + (k[1]* arctan (k[2]*(x − k[3]))) + (k[4]* exp (−((x − k[5])/k[6])^2)) + (k[7]* exp (−((x − k[8])/k[9]^2)), where x is the X-ray energy in eV and the k's are the fit parameters.

16. Kalkowski, G., Kaindl, G., Bertram, S., Schmiester, G., Rebizant, J., Spirlet, J. C. and Vogt, O., *Solid State Commun.*, 1987, **64**, 193.

17. Kalkowski, G., Kaindl, G., Brewer, W. D. and Krone, W., *Phys. Rev. B*, 1987, **35**, 2667.

18. Conradson, S. D., Rehr, J. and Mustre De Leon, J., work in progress.

19. Agarwal, B. K., *X-ray Spectroscopy*, 2nd ed.; Springer-Verlag, Berlin (1991).

20. Ghatikar, M. N. and Padilia, B. D., *J. Phys. C*, 1978, **11**, 1941.